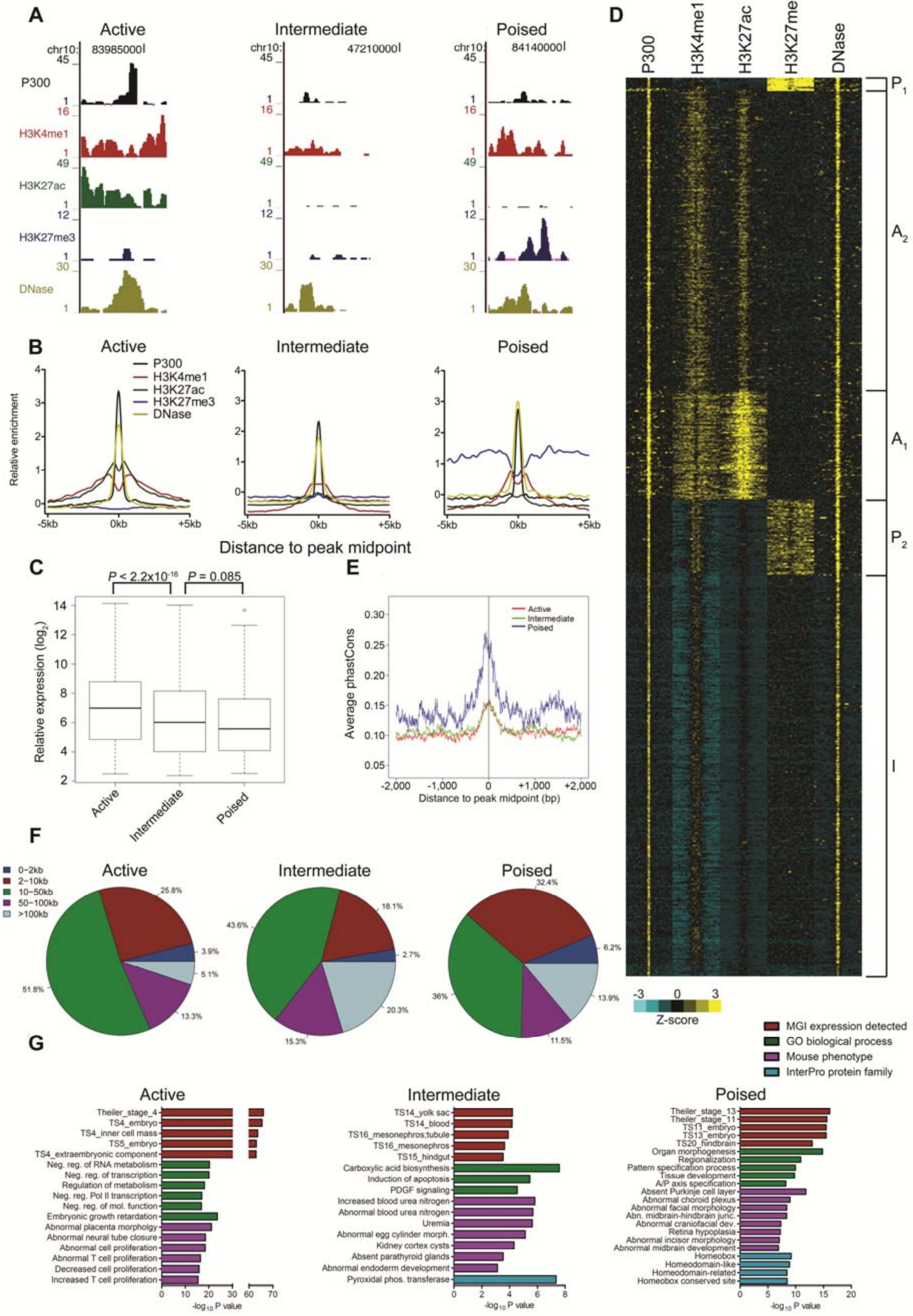
A
Active
Intermediate
Poised
chr10:
83985000
47210000
84140000
45
P300
1
16
H3K4me1
49
H3K27ac
12
H3K27me3
30
DNase
B
Active
Intermediate
Poised
P300
H3K4me1
H3K27ac
H3K27me3
DNase
Relative enrichment
-5kb
0kb
+5kb
Distance to peak midpoint
C
$P < 2.2\times10^{-16}$
$P = 0.085$
Relative expression ($\log_2$)
Active
Intermediate
Poised
D
P300
H3K4me1
H3K27ac
H3K27me3
DNase
P_1
A_2
A_1
P_2
I
-3
0
3
Z-score
E
Average phastCons
Active
Intermediate
Poised
-2,000
-1,000
0
+1,000
+2,000
Distance to peak midpoint (bp)
F
0–2kb
2–10kb
10–50kb
50–100kb
>100kb
Active
25.8%
3.9%
5.1%
13.3%
51.8%
Intermediate
18.1%
2.7%
20.3%
15.3%
43.6%
Poised
32.4%
6.2%
13.9%
11.5%
36%
G
MGI expression detected
GO biological process
Mouse phenotype
InterPro protein family
Active
Theiler_stage_4
TS4_embryo
TS4_inner cell mass
TS5_embryo
TS4_extraembryonic component
Neg. reg. of RNA metabolism
Neg. reg. of transcription
Regulation of metabolism
Neg. reg. Pol II transcription
Neg. reg. of mol. function
Embryonic growth retardation
Abnormal placenta morphology
Abnormal neural tube closure
Abnormal cell proliferation
Abnormal T cell proliferation
Decreased cell proliferation
Increased T cell proliferation
$-\log_{10}$ P value
Intermediate
TS14_yolk sac
TS14_blood
TS16_mesonephros;tubule
TS16_mesonephros
TS15_hindgut
Carboxylic acid biosynthesis
Induction of apoptosis
PDGF signaling
Increased blood urea nitrogen
Abnormal blood urea nitrogen
Uremia
Abnormal egg cylinder morph.
Kidney cortex cysts
Absent parathyroid glands
Abnormal endoderm development
Pyroxidal phos. transferase
$-\log_{10}$ P value
Poised
Theiler_stage_13
Theiler_stage_11
TS11_embryo
TS13_embryo
TS20_hindbrain
Organ morphogenesis
Regionalization
Pattern specification process
Tissue development
A/P axis specification
Absent Purkinje cell layer
Abnormal choroid plexus
Abnormal facial morphology
Abn. midbrain-hindbrain junc.
Abnormal craniofacial dev.
Retina hypoplasia
Abnormal incisor morphology
Abnormal midbrain development
Homeobox
Homeodomain-like
Homeodomain-related
Homeobox conserved site
$-\log_{10}$ P value

Supplementary Figure 1. Characteristics of p300-bound enhancers in mESCs

(A) Example ChIP-seq profiles of each enhancer class in mESCs. Data were visualized using the UCSC genome browser. (B) Aggregate plots of CHD7, H3K4me1, H3K27ac, H3K27me3, and DNase hypersensitivity signal centered on the CHD7 peak midpoint. (C) Average expression of genes associated with each enhancer class. *P*-values were calculated by Wilcoxon rank-sum test. (D) Heatmap of CHD7-bound enhancers generated by k-means cluster analysis. Each window represents signal +/- 5 kb of the CHD7 peak midpoint. Active clusters are designated A1-2, the intermediate cluster is designated I, and the poised clusters are designated P1-2. (E) Average phastCons plot for each enhancer class in a 4 kb window centered on the CHD7 peak midpoint. (F) Distribution of enhancers in each class relative to known transcription start sites. (G) Results of functional annotation of each enhancer class using GREAT. The $-\log_{10}$ of the binomial test *P*-value is reported.

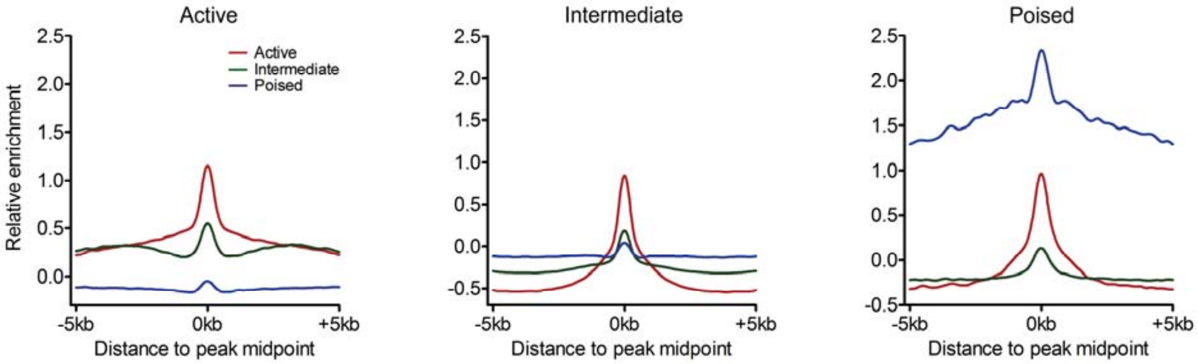

Supplementary Figure 2. Chromatin characteristics of H3K4me1/H3K27ac-defined enhancers in mESCs

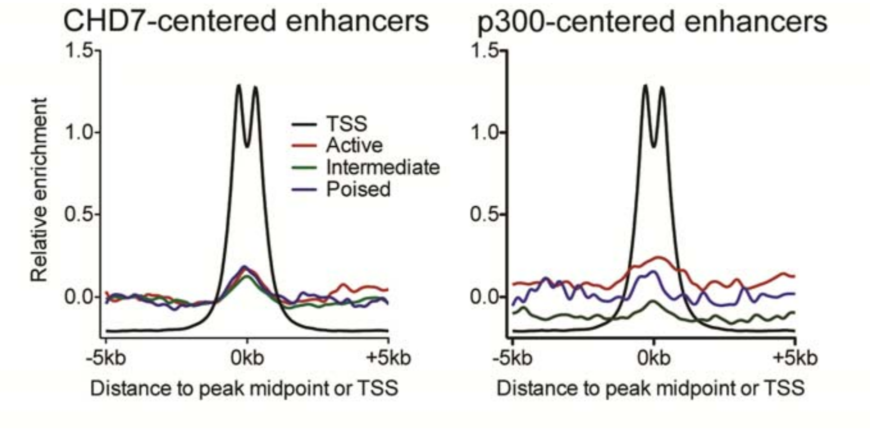

Supplementary Figure 3. Profiles of H3K4me3 signal at enhancer classes in mESCs

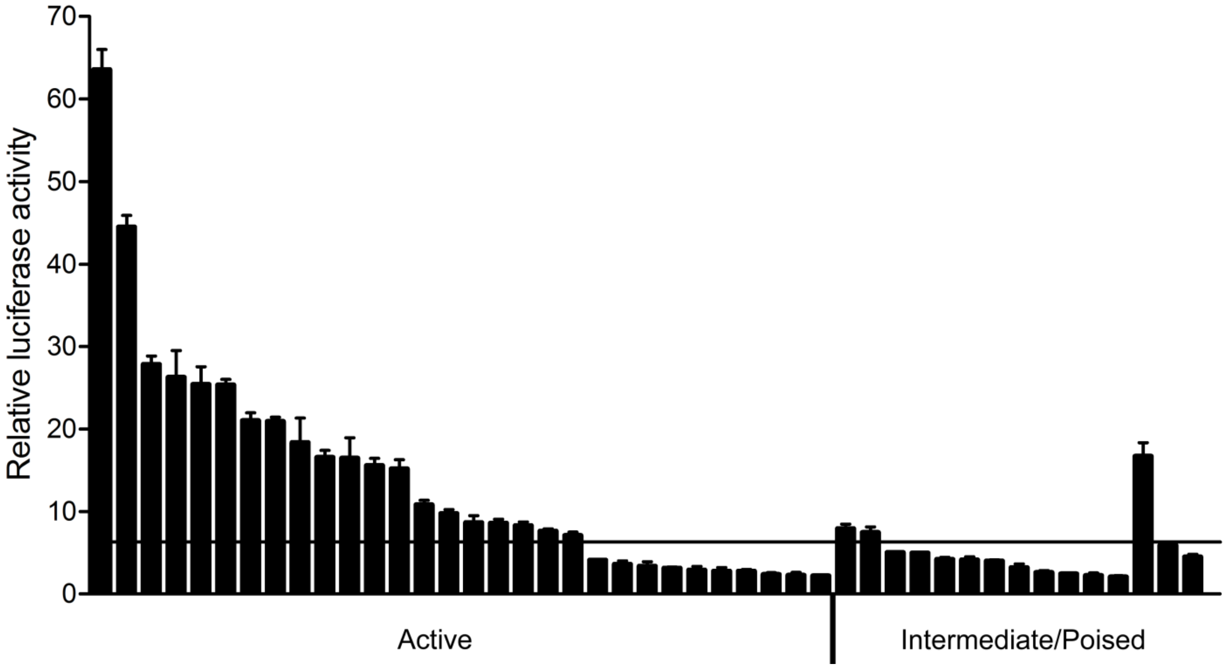

Supplementary Figure 4. Activity of computationally identified enhancers in mESCs Luciferase assay data was previously published (Schnetz et al. 2010). The threshold is set at a three-fold increase over negative controls (relative luciferase = 6.3).

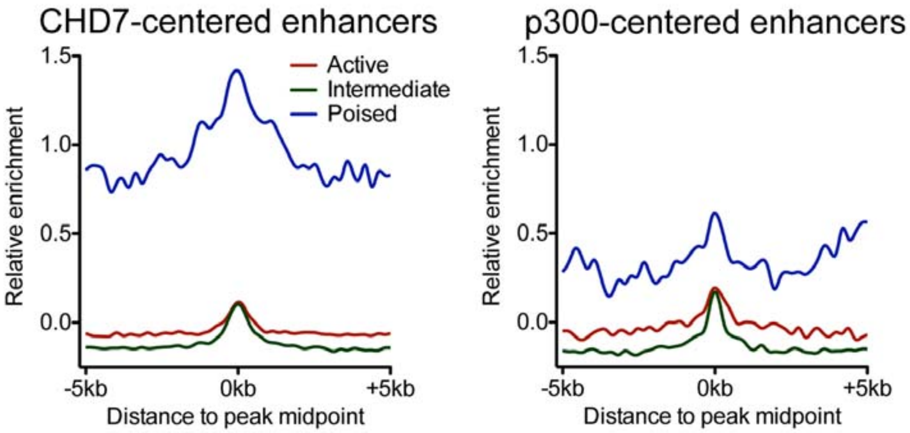

Supplementary Figure 5. Profiles of Ezh2 enrichment at enhancer classes in mESCs
Similar results were obtained after analysis of Suz12 and Ring1b ChIP-seq data (data not shown).

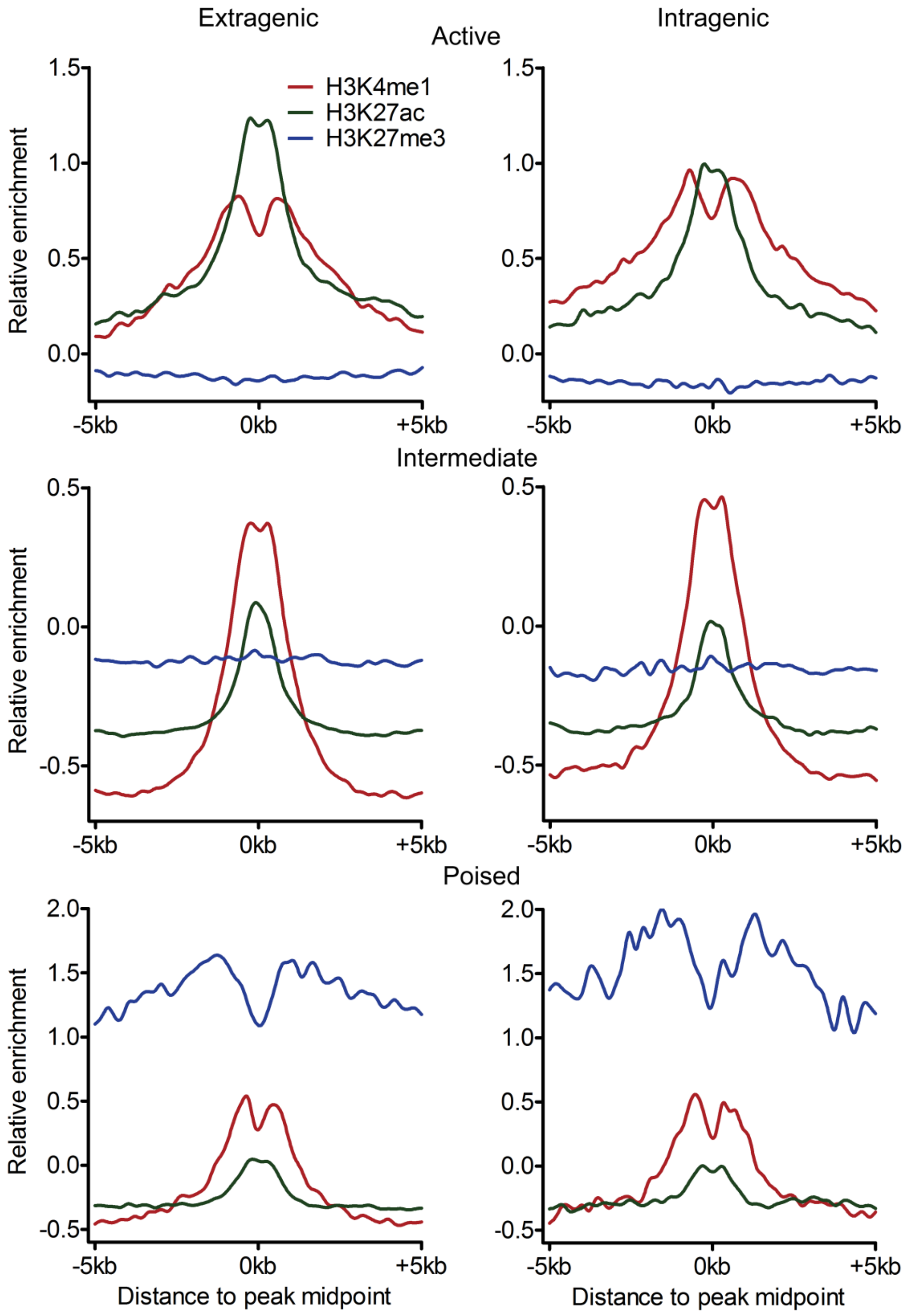

Supplementary Figure 6. Profiles of H3K4me1, H3K27ac, and H3K27me3 at extragenic and intragenic CHD7-bound mESC enhancers

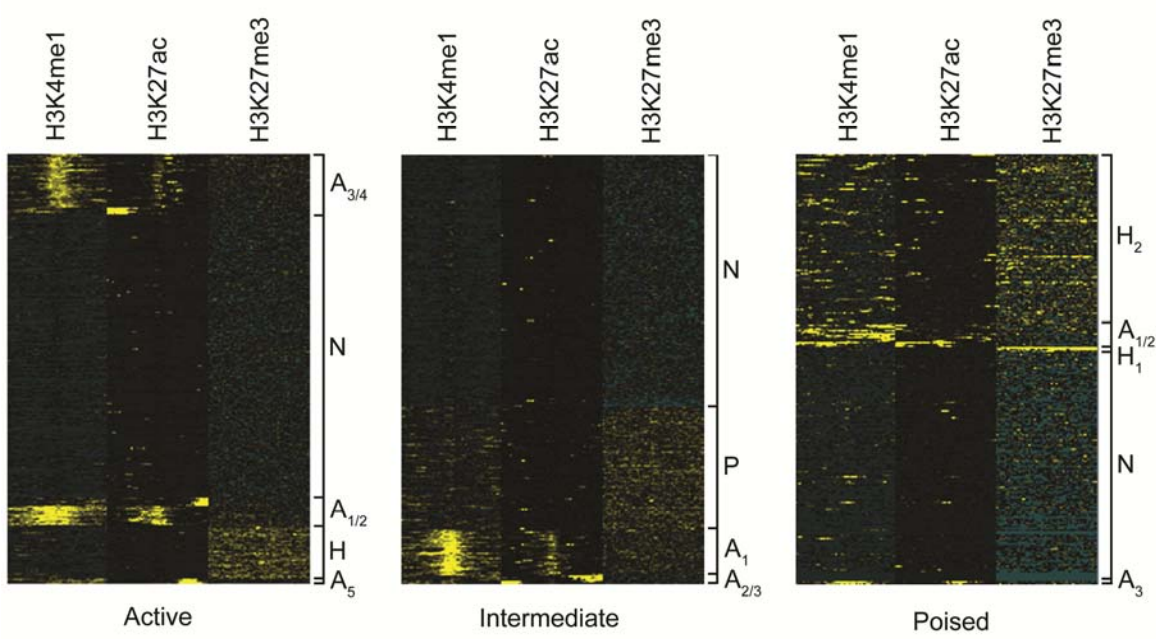

Supplementary Figure 7. Heatmap representations of mNPC enhancer classes derived from p300-bound mESC classes

Heatmaps are as described in Fig. 5A. The class of mESC enhancer from which each mNPC heatmap was generated is indicated below the heatmap. Note that, similar to CHD7-bound enhancers, both the active and poised classes give rise to active, neutral, and H3K27me3-only classes in mNPCs while intermediate enhancers give rise to active, neutral, and poised classes.

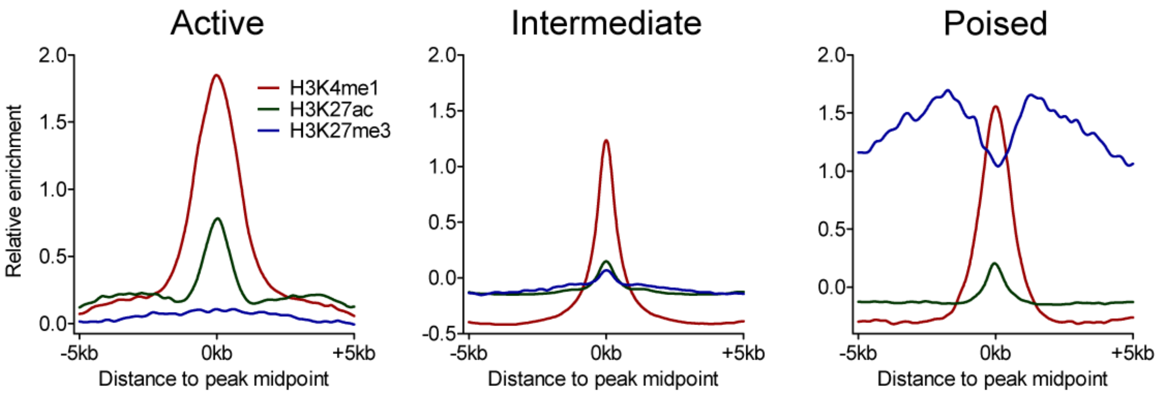

Supplementary Figure 8. Chromatin characteristics of H3K4me1/H3K27ac-defined enhancers in mNPCs

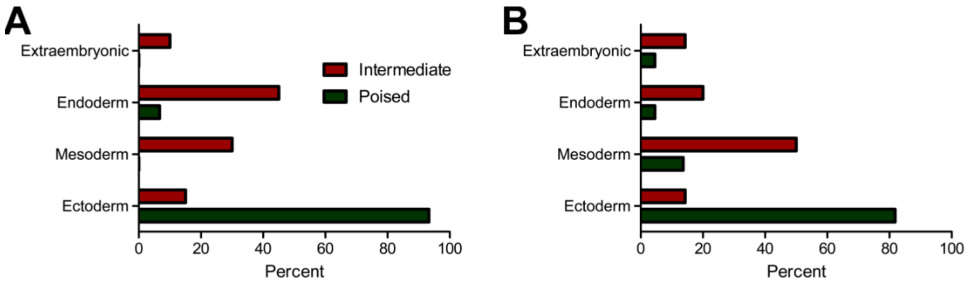

Supplementary Figure 9. GREAT analysis of non-CHD7 or -p300 centered mESC enhancers

GREAT analysis was performed as in Fig. 6, but instead of centering enhancers on CHD7 or p300 peak midpoints, enhancers were centered on the midpoints of the combined H3K4me1/H3K27ac peaks list described in the Methods section. (A) Percentage of H3K4me1/H3K27ac-defined enhancer expression annotations associated with each germ layer in mESCs. (B) Percentage of H3K4me1/H3K27ac-defined enhancer mouse phenotype annotations associated with each germ layer in mESCs.